Charge separation and energy transfer in a caroteno–C_{60} dyad: photoinduced electron transfer from the carotenoid excited states†

Rudi Berera,[a] Gary F. Moore,[b] Ivo H. M. van Stokkum,[a] Gerdenis Kodis,[b] Paul A. Liddell,[b] Miguel Gervaldo,[b] Rienk van Grondelle,[a] John T. M. Kennis,*[a] Devens Gust,*[b] Thomas A. Moore*[b] and Ana L. Moore*[b]

Received 26th September 2006, Accepted 26th October 2006
First published as an Advance Article on the web 14th November 2006
DOI: 10.1039/b613971j

We have designed and synthesized a molecular dyad comprising a carotenoid pigment linked to a fullerene derivative (C–C_{60}) in which the carotenoid acts both as an antenna for the fullerene and as an electron transfer partner. Ultrafast transient absorption spectroscopy was carried out on the dyad in order to investigate energy transfer and charge separation pathways and efficiencies upon excitation of the carotenoid moiety. When the dyad is dissolved in hexane energy transfer from the carotenoid S_2 state to the fullerene takes place on an ultrafast (sub 100 fs) timescale and no intramolecular electron transfer was detected. When the dyad is dissolved in toluene, the excited carotenoid decays from its excited states both by transferring energy to the fullerene and by forming a charge-separated $C^{\bullet+}$–$C_{60}^{\bullet-}$. The charge-separated state is also formed from the excited fullerene following energy transfer from the carotenoid. These pathways lead to charge separation on the subpicosecond time scale (possibly from the S_2 state and the vibrationally excited S_1 state of the carotenoid), on the ps time scale (5.5 ps) from the relaxed S_1 state of the carotenoid, and from the excited state of C_{60} in 23.5 ps. The charge-separated state lives for 1.3 ns and recombines to populate both the low-lying carotenoid triplet state and the dyad ground state.

Introduction

Carotenoids are ubiquitous pigments in nature where they function in a variety of ways. In photosynthesis, they absorb light in the blue–green region of the solar spectrum and transfer the energy to neighboring chlorophylls, thereby increasing the absorption cross section for photosynthetically active light. They play several crucial roles in the protection of the photosynthetic apparatus including scavenging singlet oxygen and preventing its sensitization by quenching chlorophyll triplets.[1,2] Carotenoids are also involved in non-photochemical quenching (NPQ) which is an important regulatory function in photosynthesis, controlling energy flow as a function of light intensity.[3–5] They also participate in a form of cyclic electron flow in PSII reaction centers[6,7] and appear to play a role in the structure and assembly of several pigment–protein complexes in photosynthetic membranes.[1]

Fullerenes are important building blocks in artificial reaction centers and potentially as electron accumulating devices which would be valuable components in the design of catalysts for multiple electron processes.[8–10] A remarkable property of C_{60} derivatives as participants in photoinduced electron transfer reactions, when compared with natural electron acceptors such as quinones, is their small reorganization energy (λ) and low sensitivity to solvent stabilization of the ions.[10–12] Low reorganization energy results in faster forward rates at lower driving force, *e.g.*, the peak of the Marcus curve occurs at lower driving force. This is important because energy dissipated in excessive driving force is not available for useful work. Moreover, lower reorganization energies can shift charge recombination reactions further into the "Marcus inverted region" and thereby slow the rate of recombination. A low sensitivity to solvent stabilization of the ion, and therefore of the charge-separated state, allows photoinduced electron transfer to occur over a wide range of solvents and temperature conditions. One of the characteristics of fullerenes is their very weak absorption through the visible spectrum ($\varepsilon \sim 700$ M^{-1} cm^{-1}); thus C_{60} does not lend itself to efficient solar light harvesting by direct excitation in the visible region.

Through molecular design and chemical synthesis it has been possible to attach the fullerene moiety to a variety of energy and electron donors, some of which have strong absorption in the visible.[13] In this study we investigate the photophysics and photochemistry of a molecular dyad in which a synthetic carotenoid moiety is attached covalently *via* a pyrrolidine ring to a C_{60}. The carotenoid polyene provides the system with an effective antenna for light absorption at spectral regions of maximum solar irradiance and acts as a partner in photoinduced electron transfer processes. Remarkably, the charge separation process can be initiated directly from the carotenoid excited states.

Results and discussion

Steady state absorption and fluorescence excitation spectra

The structure of the dyad and that of the model carotenoid are shown in Fig. 1. The absorption spectrum of the dyad (solid line)

[a]*Department of Biophysics, Division of Physics and Astronomy, Faculty of Sciences, Vrije Universiteit, 1081 HV, Amsterdam, The Netherlands. E-mail: john@nat.vu.nl; Fax: +31 20 5987999; Tel: +31 20 5987937*
[b]*The Center for the Study of Early Events in Photosynthesis, Department of Chemistry and Biochemistry, Arizona State University, Tempe, Arizona, 85287-1604, USA. E-mail: gust@asu.edu, tmoore@asu.edu, amoore@asu.edu; Fax: +1 480 965 2747; Tel: +1 480 965 3461*
† Electronic supplementary information (ESI) available: Time-resolved spectroscopic data and analysis. See DOI: 10.1039/b613971j

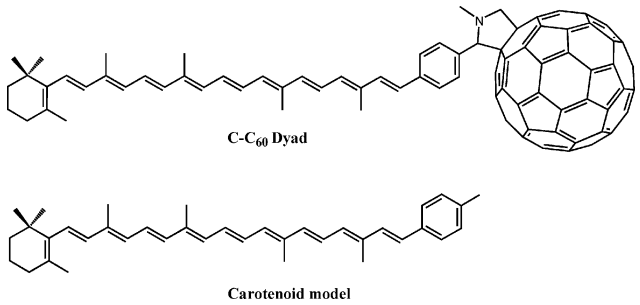

Fig. 1 Structures of the dyad and model carotenoid.

along with the absorption of the model carotenoid (dashed line) dissolved in toluene are shown in Fig. 2. The absorption spectrum of the dyad displays maxima at 450, 477.5 and 509 nm originating from vibrational levels of the carotenoid $S_0 \rightarrow S_2$ transition. The fullerene has maxima at 333 and 705 nm and absorbance at all intervening wavelengths. The model carotenoid displays maxima at 302.5, 367.5, 450, 477.5 and 509 nm.

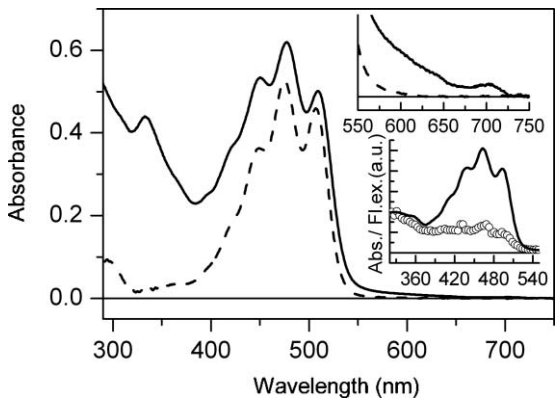

Fig. 2 Absorption spectra of $C–C_{60}$ dyad (solid line) and of the model carotenoid (dashed line) in toluene. The upper inset shows the expanded absorption spectra. The lower inset shows the absorption (solid line) and fluorescence excitation (circles) spectra in hexane.

Fluorescence excitation measurements were performed to measure the efficiency of singlet–singlet energy transfer from the carotenoid to the fullerene fluorophore. The corrected fluorescence excitation spectrum of the dyad in hexane, measured with detection at 710 nm in an optically dilute solution (optical density <0.05 at the maximum) and normalized to the absorption at 320 nm, is presented in Fig. 2 lower inset. Direct fluorescence from the carotenoid model compound is extremely weak, and is not observable under these conditions. Using these normalized spectra, the yield of singlet energy transfer was determined from the ratio of the corrected fluorescence excitation spectrum to the absorption of the dyad in the range of 420–530 nm, after first subtracting the absorption spectrum of fullerene from both spectra. The ratio (average quantum yield of energy transfer) in this range is 0.25 ± 0.05.

Femtosecond transient absorption spectroscopy

Model carotenoid: sequential analysis

Fig. 3 shows the results from a global analysis of the time-resolved data for the model carotenoid dissolved in toluene. Three

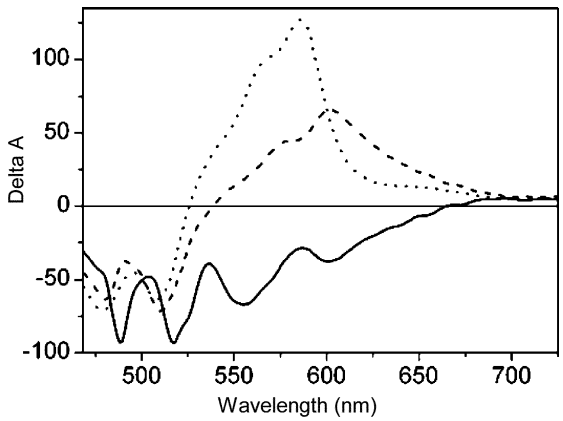

Fig. 3 Evolution associated difference spectra (EADS) that follow from the global analysis of the time-resolved experiments on the model carotenoid in toluene with excitation at 475 nm. Lifetimes: 100 fs (solid line, fixed), 300 fs (dashed line) and 7.6 ps (dotted line).

kinetic components are necessary for a good fit of the data. The first evolution associated difference spectrum (EADS, solid line) appearing at time zero presents the bleach of the carotenoid ground state at wavelengths shorter than ~525 nm as well as stimulated emission (550–670 nm), and results from population of the optically allowed S_2 state. In this global analysis, the first EADS decays to the second EADS (dashed line) in 100 fs (fixed in the global analysis since the IRF does not allow us to accurately estimate the S_2 lifetime). The second EADS displays a bleach of the carotenoid ground state below 525 nm and a region of excited state absorption with a maximum near 610 nm. Its shape has the typical profile of the hot $S_1 \rightarrow S_n$ transition; thus we assign this EADS to population of the vibrationally hot S_1 state. The third EADS (dotted line) appears after 300 fs. Compared to the previous EADS, the $S_1 \rightarrow S_n$ absorption has narrowed and blue-shifted to 590 nm, corresponding to the vibrational cooling of the hot S_1 state.[17,18] The third EADS thus corresponds to the vibrationally relaxed S_1 state. The lifetime of the S_1 state is 7.6 ps, which is comparable to the lifetime of the S_1 state for a carotenoid with an effective conjugation length between 10 and 11 conjugated double bonds.[2]

Caroteno–C_{60} dyad in hexane: sequential analysis

The result of a global analysis employing a sequential model for the dyad dissolved in hexane is shown in Fig. 4. Six components are needed for a good fit of the data: the first EADS (black line) appearing at time zero exhibits carotenoid ground state bleach and stimulated emission below 650 nm. This EADS decays into the second EADS (red line) in 100 fs (fixed in the analysis). The second EADS shows a bleach of the ground state of the carotenoid below 530 nm, as well as $S_1 \rightarrow S_n$ absorption by the vibrationally excited S_1 state. Thus, as for the model carotenoid, we assign this EADS to the vibrationally hot S_1 state. The second EADS evolves into the third EADS (green line) in 1.2 ps. The third EADS exhibits an $S_1 \rightarrow S_n$ absorption similar to that of the previous EADS, but with an overall loss of amplitude, especially in the red region. This EADS thus corresponds to the vibrationally relaxed carotenoid S_1 state. Its lifetime, 7.9 ps, is comparable to that observed for the model carotenoid. The fourth EADS (dark blue line) presents

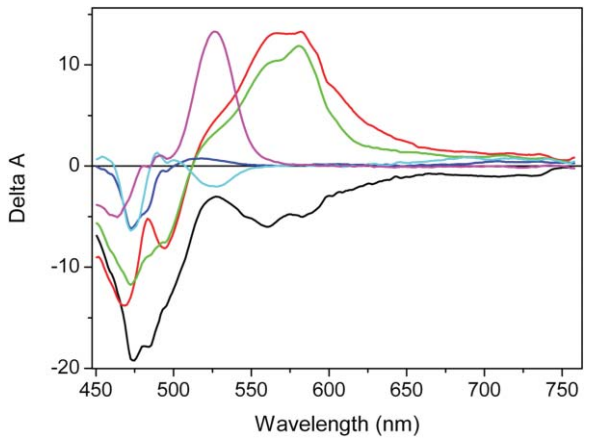

Fig. 4 Evolution associated difference spectra (EADS) that follow from the global analysis of the time-resolved experiments on the C–C_{60} dyad in hexane with excitation at 475 nm. Lifetimes: 100 fs (black line, fixed), 1.2 ps (red line), 7.9 ps (green line), 1 ns (blue line), 1ns (cyan line), and non-decaying (magenta line).

overall small amplitude (and includes a dip around 475 nm which can be assigned to a scatter contribution from the pump beam). The absence of any carotenoid ground state bleach suggests that no charge separation has taken place in the system, and that this EADS is not characteristic of the carotenoid component. The fourth EADS is thus associated with the fullerene singlet excited state, populated *via* energy transfer from the carotenoid (the C_{60}* spectral signature is small, and although formed on the fs time scale from S_2, it is only identifiable in the fourth EADS as the obscuring states disappear). A comparison of the lifetimes of the EADS corresponding to the hot S_1 and S_1 states with those obtained for the model carotenoid indicates that energy transfer to the fullerene takes place from the carotenoid S_2 state only. The fourth EADS decays to the fifth one (cyan line) in about 1 ns. The evolution is small and has a lifetime similar to that of the excited singlet state of model fullerenes. It is likely associated with singlet to triplet intersystem crossing within the C_{60} moiety. The fifth EADS decays to the final long lived EADS (magenta line), which shows a region of negative signal below 500 nm originating from the carotenoid ground state bleach, and a pronounced excited state absorption near 520 nm characteristic of the carotenoid $T_1 \rightarrow T_n$ transition. The fifth lifetime of about 1 ns thus corresponds to the time constant for energy transfer from the C_{60} triplet state to the carotenoid triplet (possibly limited by intersystem crossing in the fullerene). The final EADS (magenta line) corresponds to the lowest carotenoid triplet, populated *via* energy transfer from the C_{60} triplet state (*vide infra*). The occurrence of two sequential kinetic components with similar lifetimes and small amplitude (the fourth and fifth EADS) is related to the rise behavior of the carotenoid triplet (see Electronic Supplementary Information, ESI†).

Caroteno–C_{60} dyad in hexane: target analysis

The global analysis of the data allows one to extract the intrinsic lifetimes of the various processes but the spectra (EADS) obtained do not in general portray the spectral signature of pure molecular species. In order to extract the spectra of pure molecular species a target analysis was applied to the data.[15] In target analysis, the spectro-temporal data are described in terms of a kinetic scheme, where the rates and branchings by which molecular species interconvert are estimated. Fig. 5 shows the kinetic scheme applied to the C–C_{60} dyad in hexane. From the initially excited carotenoid S_2 state, internal conversion (IC) to 'hot S_1' takes place with a rate constant k_1, in competition with energy transfer to yield C_{60}* with rate constant k_2 and a yield of 25% (obtained from fluorescence excitation and fixed in the analysis). 'Hot S_1' vibrationally cools with rate constant k_5 to result in the relaxed S_1 state and does not contribute to the energy transfer to the fullerene. Both 'hot S_1' and S_1 have an IC rate to the ground state of k_4. The C_{60}* undergoes ISC to the triplet state $^TC_{60}$ with an efficiency of 100% (rate constant k_{10}), and triplet–triplet energy transfer from $^TC_{60}$ to the carotenoid triplet state ^TC occurs with rate constant k_8. The model also takes into account an estimated 7% direct excitation of the fullerene moiety.

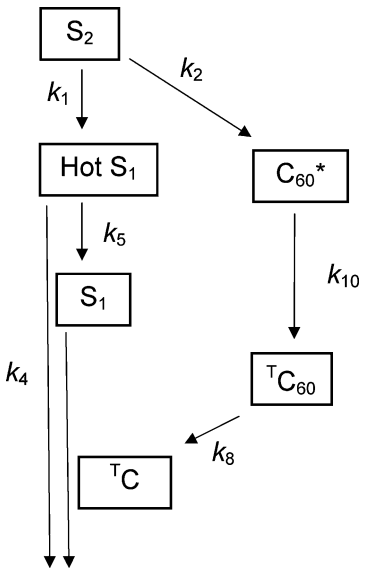

Fig. 5 Target kinetic model applied for the data of the dyad in hexane.

Fig. 6 shows the species-associated difference spectra (SADS) that follow from the target analysis, whereas the rate constants are summarized in the first column of Table 1. The S_2 (black line), hot S_1 (red line) and S_1 (green line) states of the carotenoid exhibit spectral shapes similar to those seen in the model carotenoid

Table 1 Rate constants from the target analysis of the data for the C–C_{60} dyad in hexane and toluene

Rate constant/ns^{-1}	Hexane	Toluene
k_1	7500[a]	7500[a]
k_2	2500[a]	2500[a]
k_3	0	1886
k_4	124	140
k_5	640	2891
k_6	0	35
k_7	0	35
k_8	1.4	0.09
k_9	0	0.76
k_{10}	0.8333[a]	0

[a] Fixed parameters, the estimated error in the parameters is ~10%.

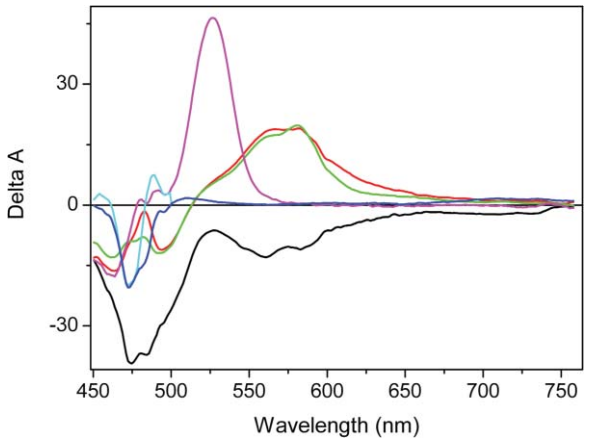

Fig. 6 Species associated difference spectra (SADS) that follow from the target analysis of the time-resolved data on the C–C_{60} dyad in hexane with excitation at 475 nm. The spectra are described in the text.

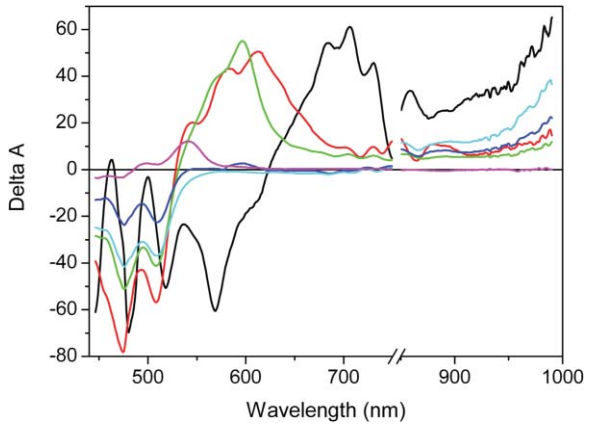

Fig. 7 Evolution associated difference spectra (EADS) that follow from the global analysis of the time-resolved experiments on the C–C_{60} dyad in toluene with excitation at 475 nm. Lifetimes: 84 fs (black line), 330 fs (red line), 5.5 ps (green line), 23.5 ps (blue line), 1.3 ns (cyan line), and non-decaying (magenta line).

(Fig. 3) and other carotenoids.[2] The C_{60}* and $^{T}C_{60}$ (blue line) states are spectrally nearly silent, with only a pump scattering contribution at 475 nm. The amplitude of the main absorption band of ^{T}C (magenta line) is twice that of the S_1 state, which is reasonable compared to values reported in the literature for a number of carotenoids.[19,20] In this model, it is assumed that the energy transfer efficiency from carotenoid to C_{60} is 25% (as measured experimentally), and that all transfer originates from S_2. This assumption is based on the fact that the lifetime of the S_1 state is basically identical in the dyad and in the model carotenoid. Unfortunately, we do not have the time resolution to measure S_2 lifetimes with and without C_{60} attached in order to verify this assumption. Taking into account the 7% direct excitation of the fullerene moiety which gives 100% triplet yield, and that 93% of the light was absorbed by the carotenoid, the total triplet yield is 30%. It is interesting to note that the SADS obtained from the target analysis are very similar in shape to the EADS obtained from the sequential analysis of the data. The reason for this resides in the fact that the two fullerene spectra considered in the target kinetic model are nearly silent.

Caroteno–C_{60} dyad in toluene: global analysis

The results from a global analysis of the time-resolved data for the dyad dissolved in toluene are shown in Fig. 7. Six components are needed for a good fit of the data: the first component (black line) appearing at time zero exhibits carotenoid ground state bleach and stimulated emission below 650 nm as well as excited state absorption features (around 475 nm the spectrum is distorted due to excitation artifacts; the feature centered at 700 nm is most likely an artifact arising from technical difficulties with the measured instrument response function). In the near IR region the EADS presents a pronounced excited state absorption from the carotenoid S_2 state.[21] This EADS decays into the second one in 84 fs (fixed in the analysis to account for the energy and electron transfer processes arising from S_2 *vide infra*). The second EADS (red line) shows the bleach of the ground state of the carotenoid below 530 nm, as well as the absorption of the hot $S_1 \rightarrow S_n$ transition and evolves into the third one (green line) in 330 fs. The third EADS has the typical shape of the carotenoid S_1 state in the visible region with ground state bleach below 530 nm and $S_1 \rightarrow S_n$ excited state absorption in the 530 to 750 nm region.

The transient absorption in the 900 to 1000 nm region in this EADS is likely to originate from a species different from the carotenoid S_1 state, most likely a carotenoid radical cation and fullerene radical anion, since the carotenoid S_1 state of this type of polyene is expected to give very low absorption around 980 nm. This suggests that some of the charge-separated state $C^{\bullet+}$–$C_{60}^{\bullet-}$ is being produced at this stage. The third spectrum decays into the next one (blue) in 5.5 ps. At this point the carotenoid S_1 state has completely decayed. The rise of the induced absorption around 980 nm is ascribed to the formation of the charge-separated state from the carotenoid S_1 state. Although the signal in the near IR region could be partially due to the C_{60} excited state, unequivocal evidence of the presence of the charge-separated state is provided by the presence of the carotenoid ground state bleach after the complete decay of the S_1 state (blue line). Thus, a $C^{\bullet+}$–$C_{60}^{\bullet-}$ state is formed directly from carotenoid excited state(s). The next evolution takes place in 23.5 ps (blue to cyan) and is characterized by an increase of the carotenoid bleach (below 550 nm) and a concomitant increase of the signal in the 900 to 1000 nm region. This is a clear indication of the formation of a charge-separated state on this timescale. The increase of the carotenoid ground state bleach means that the charge-separated state is not formed from the carotenoid, but from the fullerene, which has been excited both directly (we estimate a 7% direct fullerene excitation at 475 nm) and *via* energy transfer from the carotenoid. This EADS decays to the non-decaying component (magenta line) in 1.3 ns. This last spectrum shows a region of negative signal below 500 nm originating from the carotenoid ground state bleach and the typical carotenoid $T_1 \rightarrow T_n$ excited state absorption in the 500 to 600 nm region. At the same time the signal in the near IR region has completely disappeared, meaning that the charge-separated state has by now completely decayed. We assign this spectrum to the carotenoid triplet state. The presence of the carotenoid triplet state following the decay of the charge-separated state suggests that the charge-separated state decays at least partly to the carotenoid triplet. The only other pathway for carotenoid triplet formation, intersystem crossing in C_{60} followed

by triplet–triplet energy transfer to the carotenoid, is negligible given the short singlet lifetime of the C_{60} in the dyad.

Caroteno–C_{60} dyad in toluene: target analysis

If we suppose that the energy transfer pattern in the C–C_{60} dyad is solvent independent, the energy transfer model for the dyad in hexane provides us with the necessary information for the determination of the various pathways and relative efficiencies for charge separation in toluene. Thus, for the target analysis in toluene we have used the excitation energy transfer pathways and rate constants obtained in hexane. The target kinetic model is depicted in Fig. 8 (the rate constants are summarized in Table 1) and consists of 6 compartments: the S_2 state relaxes to a hot S_1 state with a rate constant k_1 and transfers energy to the fullerene with a rate constant k_2. Unlike the dyad in hexane, another decay channel is present for S_2, leading to the formation of the charge-separated state with a rate constant k_3. Again, we note that we cannot estimate the S_2 lifetimes. We can, however, estimate the relative rates of $S_2 \rightarrow S_1$ IC, energy transfer from S_2 to C_{60} and electron transfer from S_2 to C_{60} because those will determine the relative amounts of these primary products later on in the spectral evolution beyond the instrument response function. The hot S_1 state relaxes to the ground state with a rate constant k_4, to the relaxed S_1 state (k_5) and to directly produce the charge-separated state (k_6). The S_1 state decays partly to the ground state (k_4) and produces the charge-separated state $C^{\bullet+}$–$C_{60}^{\bullet-}$ (k_6). The excited fullerene singlet state C_{60}* decays entirely to the $C^{\bullet+}$–$C_{60}^{\bullet-}$ state with a rate constant k_7. The $C^{\bullet+}$–$C_{60}^{\bullet-}$ state decays to the carotenoid triplet with a rate constant k_8 and to the ground state with a rate constant k_9. Thus, compared to the model applied to the hexane data, four new decay channels have been added: charge separation from the carotenoid S_2, hot S_1 and S_1 states, as well as from the excited fullerene singlet state C_{60}*.

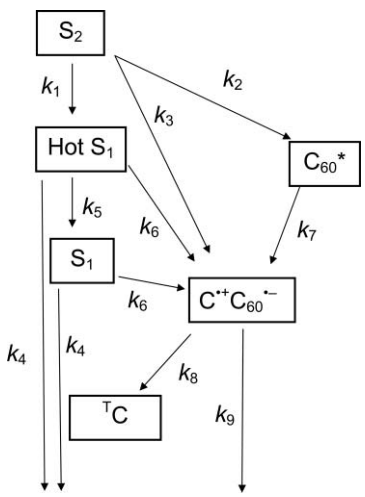

Fig. 8 Target kinetic model applied for the data in toluene.

As mentioned above, the energy transfer pathways and rate constants found in hexane are used as the "reference" for energy transfer in the dyad. With this assumption target analysis in toluene was used to find the electron transfer efficiencies based upon the correct amplitudes of the various SADS. This allows us to accurately determine the electron transfer efficiencies from the S_2, hot S_1, S_1 and C_{60}* excited states; in fact, the strict constraints imposed by the energy transfer efficiencies leaves us with a unique set of parameters for the electron transfer efficiencies that fit the data. Additionally, in the model we set the following constraints: the lifetime of the carotenoid S_2 state is fixed, the S_2 and hot S_1 SADS are set to be equal below 520 nm, and the S_1 spectrum is set to be zero above 860 nm. The model also takes into account the direct (7%) fullerene excitation.

A few representative traces at single wavelengths along with the corresponding fits from the target analysis are shown in Fig. 3 of the ESI† and illustrate the excellent quality of the fit of the model to the data. The SADS obtained from the target analysis are shown in Fig. 9 and the rate constants are summarized in Table 1. The black spectrum corresponds to the carotenoid S_2 state with ground state bleach and stimulated emission below 650 nm and a region of excited state absorption in the 650–750 nm region as well as in the near IR region. The S_2 state relaxes to the hot S_1 state with a rate constant k_1 (7500 ns^{-1}), transfers energy to the C_{60} ($k_2 = 2500\ ns^{-1}$) and produces the charge-separated state with a rate constant k_3 of 1886 ns^{-1} and a yield of 16%. The SADS corresponding to the hot S_1 state (red line) displays the bleach of the carotenoid ground state below 530 nm and the excited state absorption originating from the hot $S_1 \rightarrow S_n$ transition in the 530 to 750 nm region. The hot S_1 state also features a low excited state absorption in the near IR region (850 to 980 nm). It relaxes to the S_1 state in 2891 ns^{-1} (k_5) and to the ground state ($k_4 = 140\ ns^{-1}$), and produces the charge-separated state in very small yield with a rate constant k_6 of 35 ns^{-1}. The green line corresponds to the SADS of the carotenoid S_1 state with ground state bleach below 530 nm and excited state absorption corresponding to the $S_1 \rightarrow S_n$ transition in the 530 to 750 nm region. The S_1 state decays to the ground state (rate constant $k_4 = 140\ ns^{-1}$) and produces a charge-separated state with a rate constant k_6 (35 ns^{-1}) and a yield of 13%. The spectrum corresponding to the fullerene excited singlet state C_{60}* is in blue. It shows a characteristic induced absorption band in the 700–1000 nm region, as well as a small bleach band around 690 nm. In the carotenoid ground state absorption region a band-shift like signal is seen; this characteristic spectrum has been detected in other artificial light harvesting systems[5] and is likely to originate from a perturbation of the carotenoid ground

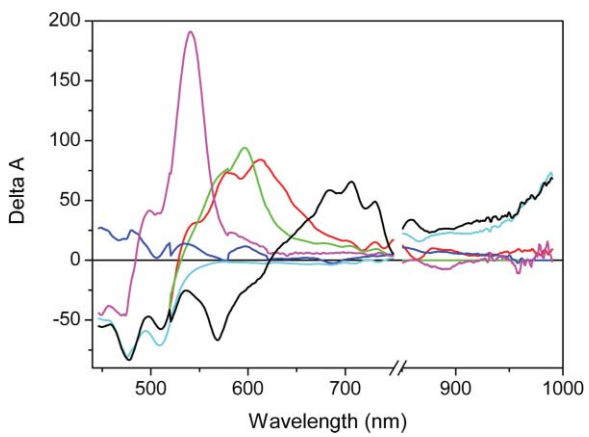

Fig. 9 Species associated difference spectra (SADS) that follow from the target analysis of the time-resolved experiments on the C–C_{60} dyad in toluene with excitation at 475 nm. The spectra are described in the text.

state due to the proximity of the excited C_{60}. C_{60} produces the charge-separated state with a rate constant k_7 (35 ns^{-1}) and a yield of 100%. The charge-separated state $C^{\bullet+}$–$C_{60}^{\bullet-}$ (cyan line) displays the carotenoid ground state bleach below 600 nm and the typical absorption of the carotenoid radical cation in the near IR region. The signal in the near IR region stems from both the carotenoid radical cation and fullerene anion but given the low extinction coefficient of the fullerene anion, about ten times smaller than the extinction coefficient of the carotenoid radical,[22,23] the predominant contribution to the spectrum comes from the carotenoid radical cation absorption. The charge-separated state recombines to populate the carotenoid triplet state (rate constant $k_8 = 0.08\ ns^{-1}$) and decays to the ground state ($k_9 = 0.76\ ns^{-1}$). The triplet state (magenta line) shows carotenoid ground state bleach below 500 nm and the typical carotenoid $T_1 \rightarrow T_n$ excited state absorption in the 500 to 650 nm region.

From our analysis the total yield of photoinduced charge separation from the carotenoid excited states is 29%, based on light absorbed by the carotenoid (which is 93% of the total light absorbed at the excitation wavelength), with 16% from S_2 and 13% from S_1. Because the yield of charge separation from the excited fullerene is 100%, the 21% energy transfer from carotenoid S_2 to yield the C_{60} excited singlet state adds 21% to charge separation arising from carotenoid light absorption. After adding the 7% yield of charge separation due to direct excitation of the fullerene moiety, which absorbs 7% of the light at the excitation wavelength, we obtain a total yield of charge separation of 54% (see ESI†).

Energy transfer from the excited states of the carotenoid in the dyad

The results from fluorescence excitation with the dyad dissolved in hexane show that about 25% of the carotenoid excitation is transferred to the fullerene. This energy transfer most likely occurs solely from the carotenoid S_2 excited state because the S_1 excited state is not quenched (the lifetime of the S_1 state is basically the same in the dyad in hexane and in the carotene model). In addition, the lifetime of the hot S_1 excited state in the dyad in hexane is rather long, 1.2 ps, indicating that energy transfer from hot S_1 is either very small or negligible. Furthermore a highly efficient energy transfer from hot S_1 is typically accompanied by energy transfer from the S_1 state and this is not seen in our system.[24]

Interestingly the energy transfer efficiency from the S_2 state is comparable to the carotenoid S_2 to phthalocyanine (Pc) efficiency obtained for artificial light harvesting triads.[25] Unlike Pc, the fullerene excited singlet state presents a very low extinction coefficient. Thus a Förster energy transfer mechanism would imply a much lower transfer efficiency in the C–C_{60} dyad as compared to the C_2–Pc triads. This suggests that energy transfer on such short length scales cannot be described by simple Förster theory.[26]

The lowest singlet excited state of C_{60} is energetically similar to those of Chl *a* in oxygenic photosynthesis and of phthalocyanine in a variety of artificial antenna constructs. It has been shown that in these systems, carotenoids with conjugation lengths of 10 double bonds or more do not have the ability to transfer energy to tetrapyrroles from their S_1 states, presumably as a result of a low-lying S_1 energy level compared to those of the tetrapyrroles and ensuing poor spectral overlap.[25,27] The carotenoid of the C–C_{60} dyad has an effective conjugation length between 10 and 11 double bonds, so energy transfer is not expected from the carotenoid S_1 state to C_{60} because of unfavorable energetics resulting in poor spectral overlap.

Charge separation from the excited states of the carotenoid in the dyad

The excited states of the carotenoid in the dyad (in toluene) are quenched compared to those of the dyad in hexane. Thus, in toluene they must be involved in other deactivating processes such as electron transfer to the fullerene. Target analysis of the transient measurements allowed us to assign rate constants to the conversions between transient species and quantify the yield of charge separation from the S_2 (16%) and S_1 (13%) carotenoid states; the direct charge separation from hot S_1 is negligible. It is interesting to note that direct electron transfer from a carotenoid S_2 state has been detected for a carotenoid attached to a TiO_2 nanoparticle.[28]

In addition to the observation that the lifetime of the S_1 state of the dyad in toluene is quenched relative to that of the model carotenoid in toluene and the dyad in hexane, the formation of $C^{\bullet+}$–$C_{60}^{\bullet-}$ from the S_1 state of the carotenoid in toluene is well supported by the observation that concomitant with the decay of the S_1 state we see a rise of the signal in the near IR corresponding to the formation of the charge-separated state. Conclusive evidence of direct charge separation from the carotenoid excited states is provided by the fact that the bleaching of the carotenoid ground state persists after the complete decay of the S_1 state and coexists with the induced absorption in the near IR, characteristic of the carotenoid radical cation and fullerene radical anion. After the decay of the carotenoid S_1 state an additional increase in the near IR absorption concomitant with an increase of the carotenoid ground state bleach at longer times clearly indicates the formation of a charge-separated state from the excited fullerene moiety.

Based on the large rate constant for quenching of the C_{60} singlet lifetime in the dyad dissolved in toluene, the quantum yield of charge separation from the C_{60} excited singlet state is ~100%.

A previously reported carotenoid–C_{60} dyad with different structural and thermodynamic parameters[29] was found to generate a charge-separated state from the C_{60} excited state in 800 fs; it decayed in 534 ps. The flash photolysis techniques employed in that study did not allow us to establish conclusively the direct involvement of the carotenoid excited state(s) in the electron transfer process.

Materials and methods

Spectroscopic techniques

Ground state absorption spectra were measured on a Shimadzu UV-3101PC UV-vis-NIR spectrometer. Steady state fluorescence emission and excitation spectra were measured using a Photon Technology International MP-1 fluorimeter and corrected. Excitation was produced by a 75 W xenon lamp and single grating monochromator. Fluorescence was detected at 90° to the excitation beam *via* a single grating monochromator and an R928 photomultiplier tube having S-20 spectral response operating in the single-photon-counting mode.

Femtosecond transient absorption spectroscopy was carried out with a setup previously described.[14] The output of a 1 kHz

amplified Ti:sapphire laser system (Coherent-BMI a1000) is used to drive a home-built non-collinear optical parametric amplifier. The excitation wavelength was tuned to 475 nm to selectively excite the S_2 state of the carotenoid moiety. The width of the instrument response function was about 300 fs FWHM and the energy was 100 nJ pulse^{-1}. A white light continuum, generated by focusing amplified 800 nm light on a 1 mm sapphire crystal, served as probe beam. The pump and the probe were focused on a 1 mm path length cuvette and, to avoid sample degradation and exposure of the sample to multiple laser shots, the cuvette was mounted on a shaker. The polarization between pump and probe was set to the magic angle (54.7°). The data were first analyzed globally using a sequential model.[15] The data are thus described by a small number of lifetimes and evolution associated difference spectra (EADS). Each EADS corresponds in general to a mixture of states and does not portray the spectrum of a pure state or species. In order to extract spectra of pure states or species a target analysis model was also applied to our data.[15]

Synthesis

The ^{1}H NMR spectra were recorded on Varian spectrometers at 300 or 500 MHz. Unless otherwise specified, samples were dissolved in deuteriochloroform with tetramethylsilane as internal reference. Mass spectra were obtained with a matrix-assisted laser desorption/ionization time-of-flight spectrometer (MALDI-TOF). All chemicals were purchased from Aldrich, Acros or Lancaster. Fullerene (C_{60}) was purchased from Materials and Electrochemical Research (MER) Corporation. Solvents were obtained from EM Science. Tetrahydrofuran was distilled from sodium metal and benzophenone in a nitrogen atmosphere immediately prior to use. Toluene was distilled from CaH_2 and dichloromethane was distilled from potassium carbonate. All solvents were stored over the appropriate molecular sieves prior to use. Thin layer chromatography (TLC) was done with silica gel coated glass plates from Analtech. Column chromatography was carried out using EM Science silica gel 60 with 230–400 mesh. All reactions were carried out under an argon atmosphere.

The carotenoid derivatives containing a carboxylic acid, 7′-apo-7-(4-carbomethoxyphenyl)-β-carotene, and a benzyl alcohol, 7′-apo-7-(4-hydroxymethylphenyl)-β-carotene, were prepared by published procedures.[16]

7′-Apo-7-(4-formylphenyl)-β-carotene. Activated manganese dioxide (147 mg, 1.69 mmol) was added to a solution of 7′-apo-7-(4-hydroxymethylphenyl)-β-carotene (63.0 mg, 121 μmol) in dichloromethane (15 mL). The mixture was stirred for 5 h before filtering the reaction mixture through a pad of Celite. The solvent was removed from the filtrate by distillation at reduced pressure and the residue was recrystallized from dichloromethane–methanol to give 59.6 mg of the desired carotenoid (95% yield): ^{1}H NMR (300 MHz, $CDCl_3$): δ 1.02 (6H, s, CH_3-16C and CH_3-17C), 1.44–1.48 (2H, m, CH_2-2C), 1.57–1.65 (2H, m, CH_2-3C), 1.70 (3H, s, CH_3-18C), 1.96–2.05 (14H, m, CH_3-19C, CH_3-20C, CH_3-20′C, 2H, m, CH_2-4C, and CH_3-19′C), 6.01–6.16 (3H, m, H-8C, H-10C, and H-7C), 6.22–6.43 (5H, m, H-14C, H-14′C, H-12C, H-10′C, and H-12′C), 6.62–6.71 (5H, m, H-7′C, H-11C, H-11′C, H-15C, and H-15′C), 6.65 (1H, d, J = 15.9 Hz, H-7′C), 7.01 (1H, d, J = 15.9 Hz, H-8′C), 7.53 (2H, d, J = 8.2 Hz, H-1′C and H-5′C), 7.79 (2H, d, J = 8.2 Hz, H-2′C and H-4′C), 9.94 (1H, s, CHO-21′C); MALDI-TOF-MS m/z; calcd. for $C_{38}H_{46}O$ 518.35, obsd. 518.35.

Caroteno–C_{60} dyad (C–C_{60}). A portion of C_{60} (153 mg, 212 μmol), sarcosine (94.5 mg, 1.06 mmol), 7′-apo-7-(4-formylphenyl)-β-carotene (55.0 mg, 106 μmol) and toluene (170 mL) were added to a flask fitted with a condenser. The reaction mixture was refluxed under a nitrogen atmosphere for 24 h. After cooling, the solvent was evaporated at reduced pressure and the residue was resuspended in 30% carbon disulfide in toluene and filtered. The solvent was removed from the filtrate by distillation at reduced pressure and the residue was dissolved in a mixture of carbon disulfide : toluene : hexanes (1 : 1 : 2). This mixture was applied to a silica gel column and the excess C_{60} was eluted with carbon disulfide : toluene : hexanes (1 : 1 : 2). The product was then eluted with a mixture of carbon disulfide : toluene : hexanes (1 : 1 : 1) to yield 80.6 mg of the dyad (60% yield): ^{1}H NMR (300 MHz, $CDCl_3/CS_2$): δ 0.99 (6H, s, CH_3-16C and CH_3-17C), 1.42–1.46 (2H, m, CH_2-2C), 1.57–1.62 (2H, m, CH_2-3C), 1.67 (3H, s, CH_3-18C), 1.91–1.98 (14H, m, CH_3-19C, CH_3-20C, CH_3-20′C, 2H, m, CH_2-4C, and CH_3-19′C), 2.79 (3H, s, NCH_3), 4.23 (1H, d, J = 9.3 Hz, NCH_2), 4.87 (1H, s, CH-21′C), 4.93 (1H, d, J = 9.3 Hz, NCH_2), 6.04–5.91 (3H, m, H-8C, H-10C, and H-7C), 6.05–6.34 (5H, m, H-14C, H-14′C, H-12C, H-10′C, and H-12′C), 6.37–6.66 (5H, m, H-7′C, H-11C, H-11′C, H-15C, and H-15′C), 6.78 (1H, d, J = 15.9 Hz, H-8′C), 7.35 (2H, br m, H-1′C and H-5′C), 7.69 (2H, brs, H-2′C and H-4′C); MALDI-TOF-MS m/z. calcd. for $C_{100}H_{51}N$ 1266.41, obsd. 1266.41; UV-vis (toluene) 333, 450, 477.5, 509, 705 nm.

7′-Apo-7-(4-tolyl)-β-carotene (model carotenoid). A portion of β-apo-8′-carotenal (466 mg, 1.12 mmol), 4-methylbenzyltriphenylphosphonium bromide (1.00 g, 2.24 mmol), sodium methoxide (182 mg, 3.36 mmol), and dimethylsulfoxide (55 mL) were added to a flask fitted with a condenser. The mixture was stirred under a nitrogen atmosphere for 15 h at 65 °C. The reaction was quenched by pouring the mixture into ether (110 mL) followed by washing twice with brine and four times with water. The organic layer was dried with sodium sulfate and filtered, and the solvent was evaporated at reduced pressure. The residue was recrystallized twice from dichloromethane–methanol to yield 423 mg of the desired carotenoid (75% yield):^{1}H NMR (300 MHz, $CDCl_3$): δ 1.03 (6H, s, CH_3-16C and CH_3-17C), 1.44–1.50 (2H, m, CH_2-2C), 1.56–1.68 (2H, m, CH_2-3C), 1.72 (3H, s, CH_3-18C), 1.98–2.04 (14H, m, CH_3-19C, CH_3-20C, CH_3-20′C, 2H, m, CH_2-4C, and CH_3-19′C), 2.34 (3H, s, CH_3-21′C), 6.01–6.16 (3H, m, H-8C, H-10C, and H-7C), 6.22–6.43 (5H, m, H-14C, H-14′C, H-12C, H-10′C, and H-12′C), 6.56 (1H, d, J = 16.2 Hz, H-7′C), 6.62–6.71 (4H, m, H-11C, H-11′C, H-15C, and H-15′C), 6.85 (1H, d, J = 16.2 Hz, H-8′C), 7.12 (2H, d, J = 8.1 Hz, H-1′C and H-5′C or H-2′C and H-4′C), 7.32 (2H, d, J = 8.1 Hz, H-2′C and H-4′C or H-1′C and H-5′C); MALDI-TOF-MS m/z. calcd. for $C_{38}H_{48}$ 504.38, obsd. 504.36; UV-vis (CH_2Cl_2) 293, 366, 445, 474.5, 506 nm.

Conclusions

We have studied energy transfer and charge separation within a carotenoid–C_{60} light harvesting dyad. When the system is dissolved in hexane ultrafast energy transfer from the carotenoid S_2 state to the C_{60} moiety is followed by intersystem crossing within the

fullerene, after which back energy transfer to the carotenoid triplet is observed. When the system is dissolved in the more polar solvent toluene, multiple electron transfer channels become available. Our results clearly indicate that two carotenoid excited states are directly involved in the electron transfer process and that ultrafast energy transfer from the carotenoid S_2 to the C_{60} occurs with 21% efficiency (25% in hexane solution). Evolution associated decay measurements followed by target analysis indicate that the quantum yield of charge separation based on light absorbed by the carotenoid is approximately 47%, about one-half of which is due to photoinduced electron transfer from the excited carotenoid and about one-half following energy transfer from the carotenoid to the C_{60} so that the C_{60} excited singlet state initiates photoinduced hole transfer. Light absorbed by the fullerene is 100% effective in generating the charge-separated state. This genre of dyad is unique in that in other dyad systems studied to date, where the carotenoid acts as an electron donor, the charge separation process is always initiated from an excited state of the electron acceptor, either a porphyrin or a phthalocyanine.[25,30]

Acknowledgements

This work was supported by a grant from the U. S. Department of Energy (DE-FG02-03ER15393). This is publication 670 from the ASU center for the Study of early Events in Photosynthesis. R.B. was supported by the Netherlands Organization for Scientific Research through the Earth and Life Sciences Council (NWO-ALW). J.T.M.K. was supported by NWO-ALW *via* a VIDI fellowship. We thank Kate Mullen for her help in the preparation of the cover figure for this issue containing papers on fullerenes.

References

1 H. A. Frank and R. J. Cogdell, Carotenoids in photosynthesis, *Photochem. Photobiol.*, 1996, **63**, 257–264.
2 T. Polívka and V. Sundström, Ultrafast dynamics of carotenoid excited states—from solution to natural and artificial systems, *Chem. Rev.*, 2004, **104**, 2021–2071.
3 N. E. Holt, G. R. Fleming and K. K. Niyogi, Toward an understanding of the mechanism of nonphotochemical quenching in green plants, *Biochemistry*, 2004, **43**, 8281–8289.
4 N. E. Holt, D. Zigmantas, L. Valkunas, X. P. Li, K. K. Niyogi and G. R. Fleming, Carotenoid cation formation and the regulation of photosynthetic light harvesting, *Science*, 2005, **307**, 433–436.
5 R. Berera, C. Herrero, I. H. M. van Stokkum, M. Vengris, G. Kodis, R. E. Palacios, H. van Amerongen, R. van Grondelle, D. Gust, T. A. Moore, A. L. Moore and J. T. M. Kennis, A simple artificial light-harvesting dyad as a model for excess energy dissipation in oxygenic photosynthesis, *Proc. Natl. Acad. Sci. U. S. A.*, 2006, **103**, 5343–5348.
6 J. S. Vretos, D. H. Steward, J. D. de Paula and G. W. Brudvig, Low-temperature optical and resonance Raman spectra of a carotenoid cation radical in photosystem II, *J. Phys. Chem. B*, 1999, **103**, 6403–6406.
7 P. Faller, A. Pascal and A. W. Rutherford, β-Carotene redox reactions in photosystem II: electron transfer pathway, *Biochemistry*, 2001, **40**, 6431–6440.
8 P. A. Liddell, J. P. Sumida, A. N. Macpherson, L. Noss, G. R. Seely, K. N. Clark, A. L. Moore, T. A. Moore and D. Gust, Preparation and photophysical studies of porphyrin C-60 dyads, *Photochem. Photobiol.*, 1994, **60**, 537–541.
9 R. M. Williams, J. M. Zwier and J. W. Verhoeven, Photoinduced intramolecular electron-transfer in a bridged C_{60} (acceptor) aniline (donor) system-photophysical properties of the first active fullerene diad, *J. Am. Chem. Soc.*, 1995, **117**, 4093–4099.
10 D. Kuciauskas, P. A. Liddell, S. Lin, S. G. Stone, A. L. Moore, T. A. Moore and D. Gust, Photoinduced electron transfer in carotenoporphyrin–fullerene triads: temperature and solvent effects, *J. Phys. Chem. B*, 2000, **104**, 4307–4321.
11 D. M. Guldi, Fullerene-porphyrin architectures; photosynthetic antenna and reaction center models, *Chem. Soc. Rev.*, 2002, **31**, 22–36.
12 H. Imahori, K. Hagiwara, T. Akiyama, M. Aoki, S. Taniguchi, T. Okada, M. Shirakawa and Y. Sakata, The small reorganization energy of C-60 in electron transfer, *Chem. Phys. Lett.*, 1996, **263**, 545–550.
13 D. Gust, T. A. Moore and A. L. Moore, Mimicking photosynthetic solar energy transduction, *Acc. Chem. Res.*, 2001, **34**, 40–48.
14 C. C. Gradinaru, I. H. M. van Stokkum, A. A. Pascal, R. van Grondelle and H. van Amerongen, Identifying the pathways of energy transfer between carotenoids and chlorophylls in LHCII and CP29. A multicolor, femtosecond pump–probe study, *J. Phys. Chem. B*, 2000, **104**, 9330–9342.
15 I. H. M. van Stokkum, D. S. Larsen and R. van Grondelle, Global and target analysis of time-resolved spectra, *Biochim. Biophys. Acta*, 2004, **1657**, 82–104.
16 D. Gust, T. A. Moore, A. L. Moore and P. A. Liddell, Synthesis of carotenoporphyrin models for photosynthetic energy and electron-transfer, *Methods Enzymol.*, 1992, **213**, 87–100.
17 H. H. Billsten, D. Zigmantas, V. Sundström and T. Polívka, Dynamics of vibrational relaxation in the S_1 state of carotenoids having 11 conjugated C=C bonds, *Chem. Phys. Lett.*, 2002, **355**, 465–470.
18 F. L. de Weerd, I. H. M. van Stokkum and R. van Grondelle, Subpicosecond dynamics in the excited state absorption of all-*trans*-β-Carotene, *Chem. Phys. Lett.*, 2002, **354**, 38–43.
19 R. J. Cogdell, E. J. Land and T. G. Truscott, The triplet extinction coefficients of some bacterial carotenoids, *Photochem. Photobiol.*, 1983, **38**, 723–725.
20 B. R. Nielsen, K. Jørgensen and L. H. Skibsted, Triplet–triplet extinction coefficients, rate constants of triplet decay and rate constants of antracene triplet sensitization by laser flash photolysis of astaxanthin, β-carotene, canthaxanthin and zeaxanthin in deaerated toluene at 298 K, *J. Photochem. Photobiol., A*, 1998, **112**, 127–133.
21 E. Papagiannakis, I. H. M. van Stokkum, R. van Grondelle, R. A. Niederman, D. Zigmantas, V. Sundström and T. Polívka, A near-infrared transient absorption study of the excited-state dynamics of the carotenoid spirilloxanthin in solution and in the LH1 complex of Rhodospirillum rubrum, *J. Phys. Chem. B*, 2003, **107**, 11216–11223.
22 E. J. Land, D. Lexa, R. V. Bensasson, D. Gust, T. A. Moore, A. L. Moore, P. A. Liddell and G. A. Nemeth, Pulse radiolytic and electrochemical investigations of intramolecular electron-transfer in carotenoporphyrins and carotenoporphyrin quinone triads, *J. Phys. Chem.*, 1987, **91**, 4831–4835.
23 M. A. Greaney and S. M. Gorun, Production, spectroscopy, and electronic structure of soluble fullerene ions, *J. Phys. Chem.*, 1991, **95**, 7142–7144.
24 E. Papagiannakis, J. T. M. Kennis, I. H. M. van Stokkum, R. J. Cogdell and R. van Grondelle, An alternative carotenoid-to-bacteriochlorophyll energy transfer pathway in photosynthetic light harvesting, *Proc. Natl. Acad. Sci. U. S. A.*, 2002, **99**, 6017–6022.
25 G. Kodis, C. Herrero, R. Palacios, E. Marino-Ochoa, S. Gould, L. de la Garza, R. van Grondelle, D. Gust, T. A. Moore, A. L. Moore and J. T. M. Kennis, Light harvesting and photoprotective functions of carotenoids in compact artificial photosynthetic antenna designs, *J. Phys. Chem. B*, 2004, **108**, 414–425.
26 G. D. Scholes, X. J. Jordanides and G. R. Fleming, Adapting the Förster theory of energy transfer for modeling dynamics in aggregated molecular assemblies, *J. Phys. Chem. B*, 2001, **105**, 1640–1651.
27 N. E. Holt, J. T. M. Kennis and G. R. Fleming, Femtosecond fluorescence upconversion studies of light harvesting by β-carotene in oxygenic photosynthetic core proteins, *J. Phys. Chem. B*, 2004, **108**, 19029–19035.
28 J. Pan, G. Benko, Y. H. Xu, T. Pascher, L. Sun, V. Sundström and T. Polívka, Photoinduced electron transfer between a carotenoid and TiO_2 nanoparticle, *J. Am. Chem. Soc.*, 2002, **124**, 13949–13957.
29 H. Imahori, S. Cardoso, D. Tatman, S. Lin, L. Noss, G. R. Seely, L. Sereno, J. C. de Silber, T. A. Moore, A. L. Moore and D. Gust, Photoinduced electron transfer in a carotenobuckminsterfullerene dyad, *Photochem. Photobiol.*, 1995, **62**, 1009–1014.
30 R. M. Hermant, P. A. Liddell, S. Lin, R. G. Alden, H. K. Kang, A. L. Moore, T. A. Moore and D. Gust, Mimicking carotenoid quenching of chlorophyll fluorescence, *J. Am. Chem. Soc.*, 1993, **115**, 2080–2081.